Heliyon

ELSEVIER

Received:
18 July 2017
Revised:
12 October 2017
Accepted:
21 November 2017

Cite as: Diogo Montalvão, Andrew Wren. Redesigning axial-axial (biaxial) cruciform specimens for very high cycle fatigue ultrasonic testing machines.
Heliyon 3 (2017) e00466.
doi: 10.1016/j.heliyon.2017.e00466

Redesigning axial-axial (biaxial) cruciform specimens for very high cycle fatigue ultrasonic testing machines

Diogo Montalvão *, Andrew Wren

Department of Design and Engineering, Faculty of Science and Technology, Bournemouth University, Poole House, Talbot Campus, Fern Barrow, Poole BH12 5BB, UK

* Corresponding author.

E-mail address: dmontalvao@bournemouth.ac.uk (D. Montalvão).

Abstract

The necessity to increase performances in terms of lifetime and security in mechanical components or structures is the motivation for intense research in fatigue. Applications range from aeronautics to medical devices. With the development of new materials, there is no longer a fatigue limit in the classical sense, where it was accepted that the fatigue limit is the stress level such that there is no fracture up to 1E7 cycles. The recent development of ultrasonic testing machines where frequencies can go as high as 20 kHz or over enabled tests to be extended to ranges larger than 1E9 in just a few days. This area of studies is now known as Very High Cycle Fatigue (VHCF).

On the other hand, most of the existing test equipment in the market for both classical and VHCF are uniaxial test machines. However, critical components used in Engineering applications are usually subjected to complex multi-axial loading conditions.

In this paper, it is presented the methodology to redesigning existing cruciform test specimens that can be used to create an in-plane biaxial state of stress when used in 'uniaxial' VHCF ultrasonic testing machines (in this case, the term 'uniaxial' is used not because of the state of stress created at the centre of the specimen, but because of the direction at which the load is applied). The methodology is explained in such a way that it can be expanded to other existing designs, namely

http://dx.doi.org/10.1016/j.heliyon.2017.e00466

cruciform designs, that are not yet used in VHCF. Also, although the approach is presented in simple and logical terms, it may not be that obvious for those who have a more focused approach on fatigue rather than on modal analysis. It is expected that by contributing to bridging the gap between the sciences of modal analysis and fatigue, this research will help and encourage others exploiting new capabilities in VHCF.

Keywords: Materials science, Engineering, Mechanical engineering

1. Introduction

The emergence of new technologies, manufacturing processes and materials, together with the necessity to increase the lifetime and safety of mechanical systems, led to the need to increase the fatigue life range of mechanical components (Anes et al., 2011). Thus, fatigue data beyond the specific cycles is necessary to design mechanical components that will be subjected to extended lifetimes in comparison to the past (Freitas et al., 2011).

With the development of new materials, such as high strength aluminium alloys with a different microstructure from steels, materials no longer have a fatigue limit in the classical sense, where it was accepted that the fatigue limit is the stress level such that there is no fracture up to 1E7 (Freitas et al., 2011). This limit, often referred to 'infinite' fatigue life, has already been dismissed by, for example, (Bathias, 1999) and (Pyttel et al., 2011). This led to conclude the necessity to improve the S-N diagrams

and eliminate the endurance limit (Bathias, 1999; Frederick, 1965). Actually, new testing equipment allowed for the extension of the concept of fatigue up to 1E9 cycles and even more (Lage et al., 2014).

In classical fatigue testing, the machines' low operating frequencies require unfeasible lengths of time for the completion of tests up to 1E9 cycles. For example, typical rotating bending machines operate at frequencies up to 30 Hz, servo-hydraulic machines work at frequencies up to 50 Hz and resonant fatigue machines work at around 150 Hz. This means that, in order to achieve 1E9 cycles, conventional testing may require a machine to be operating between 3 months to 1 year; that is, without interruptions.

The recent development of ultrasonic testing machines where frequencies can go as high as 20 kHz or over enabled tests to be extended to ranges larger than 1E9 in a reasonable amount of time. This area of studies is now known as gigacycle or Very High Cycle Fatigue (VHCF). With a machine operating at 20 kHz the length of time required to reach 1E9 cycles could be reduced, in theory, to as little as 14 h, if no interruptions had to be made.

http://dx.doi.org/10.1016/j.heliyon.2017.e00466

On the other hand, most of the existing test equipment in the market for both classical and VHCF are uniaxial test machines (Cláudio et al., 2014a), in the sense that the state of stress created is unidirectional. However, critical components used by the aerospace, automotive, energy, naval, medical and other industries are usually subjected to complex multi-axial loading conditions (Montalvão et al., 2014; Reis et al., 2014). The market already offers two types of machines for biaxial fatigue testing: combined axial-torsion and combined in-plane axial-axial (which includes tension-tension, tension-compression or compression-compression). The first method uses thin-walled cylinder specimens (tubes), whereas the second one employs cruciform specimens (Cláudio et al., 2014a).

The combined axial-torsion test is commonly used to assess the fatigue life of shafts and similar components. However, besides allowing for only a few stress states to be simulated, it requires the material to come in the form of circular tubes, being difficult to be applied to rolled sheet and composite materials (Cláudio et al., 2014a). Nevertheless, recently, Costa et al. (2017) presented a new specimen and horn design for combined tension and torsion ultrasonic fatigue testing in the VHCF regime. Results show that it is possible to carry out multiaxial (axial/torsion loading) fatigue tests at very high frequencies.

The combined biaxial in-plane fatigue machines require that the centre of the specimen does not move during the test, which means that the four actuators must be precisely synchronised (Baptista et al., 2014; Cláudio et al., 2014a). Furthermore, the almost only available in-plane biaxial machines available so far in the market use servo-hydraulic actuators. Thus, these machines are not good candidates to be used in VHCF, due to time constraints.

In this paper, it is proposed an original approach to biaxial fatigue testing in the VHCF regime. Having as starting point the same principles used in the design of the VHCF machines as in, for example, Bathias et al. (2002), Bathias (2006), Freitas et al. (2011), Lage et al. (2012) or Lage et al. (2014), it will be shown that, at least when using cruciform specimens for in-plane axial-axial (biaxial) testing, only the specimen needs to be redesigned and no changes are required to the machine (for example, Costa et al. (2017) redesigns both the specimen and the horn for combined axial-torsion). The redesign of these specimens can be achieved by the application of a simple scale factor which, as will be shown, is inversely proportional to the change in the natural frequencies. Therefore, and in principle, any existing specimen that is already designed for in-plane axial-axial (biaxial) fatigue testing, such as typical cruciform specimens, could be scaled down (or up) so that its natural frequencies are adjusted to meet the requirements of VHCF ultrasonic test machines like the ones mentioned above. The method to redesign the specimens is presented using Finite Element Analysis (FEA) and uses, as case study, the cruciform specimens from Baptista et al. (2014). The final design is

http://dx.doi.org/10.1016/j.heliyon.2017.e00466

presented so that researchers with access to experimental testing facilities can perform experimental testing and continue research in this area.

2. Background

The basic principle behind VHCF testing machines as the ones discussed in, for example Bathias et al. (2002), Bathias (2006), Freitas et al. (2011), Lage et al. (2012) or Lage et al. (2014), is based on the resonance phenomenon. In the system shown in Fig. 1, a piezoelectric actuator introduces a pure axial harmonic vibration at 20 ± 0.5 kHz. This vibration is transmitted and amplified through a system composed by a booster (where the whole assembly is supported) and a horn, down to the specimen. These four parts form the resonant system of the testing machine. The principle of operation of the vibration system is based on free vibration resulting in a minimum of contact force between the elements in the system. Each element in the resonant system is manufactured to have the same axial fundamental frequency and vibrate in phase opposition at the contact points. Therefore, one important aspect to have into consideration is that the test specimen must be designed to have a certain mode shape tuned to the operating frequency of the machine, in this case 20 ± 0.5 kHz (19.5 ~ 20.5 kHz).

3. Design

3.1. Cruciform test specimen type and Uncalibrated Design (UD)

There have been attempts to design test specimens to create an in-plane state of biaxial stress. Typically, specimens are cruciform, as are the designs from, for example, Makris et al. (2010), Bellett et al. (2011) or Shlyannikov et al. (2014). The design from Bellett et al. (2011) has the particularity that it can be used in conventional uniaxial test machines, as it is the shape of an 'hourglass' with two 'tear-shaped' holes above and below the centreline of the specimen to generate a biaxial stress state at the centre. While this design represents a breakthrough and intelligent approach to creating a biaxial state of stress that can be used in the most conventional of the testing equipment available, it has some limitations when it comes to VHCF, as it does not allow non-proportional stresses (e.g., an in-plane biaxial state of stress where stresses have a phase shift of 180°, i.e., they are out-of-phase).

This paper will use as case study the cruciform shape shown in Fig. 2, although it is expected that the concepts can be easily transferred to other existing designs, namely cruciform designs. This shape is based on the optimised geometry proposed by Baptista et al. (2014) and Baptista et al. (2015). Specimens with a reduced thickness at the centre are used to increase the stress at the centre, so that the chances that cracks will initiate and propagate at this location increase. Also, these areas are designed to produce an uniform stress distribution at the centre

http://dx.doi.org/10.1016/j.heliyon.2017.e00466

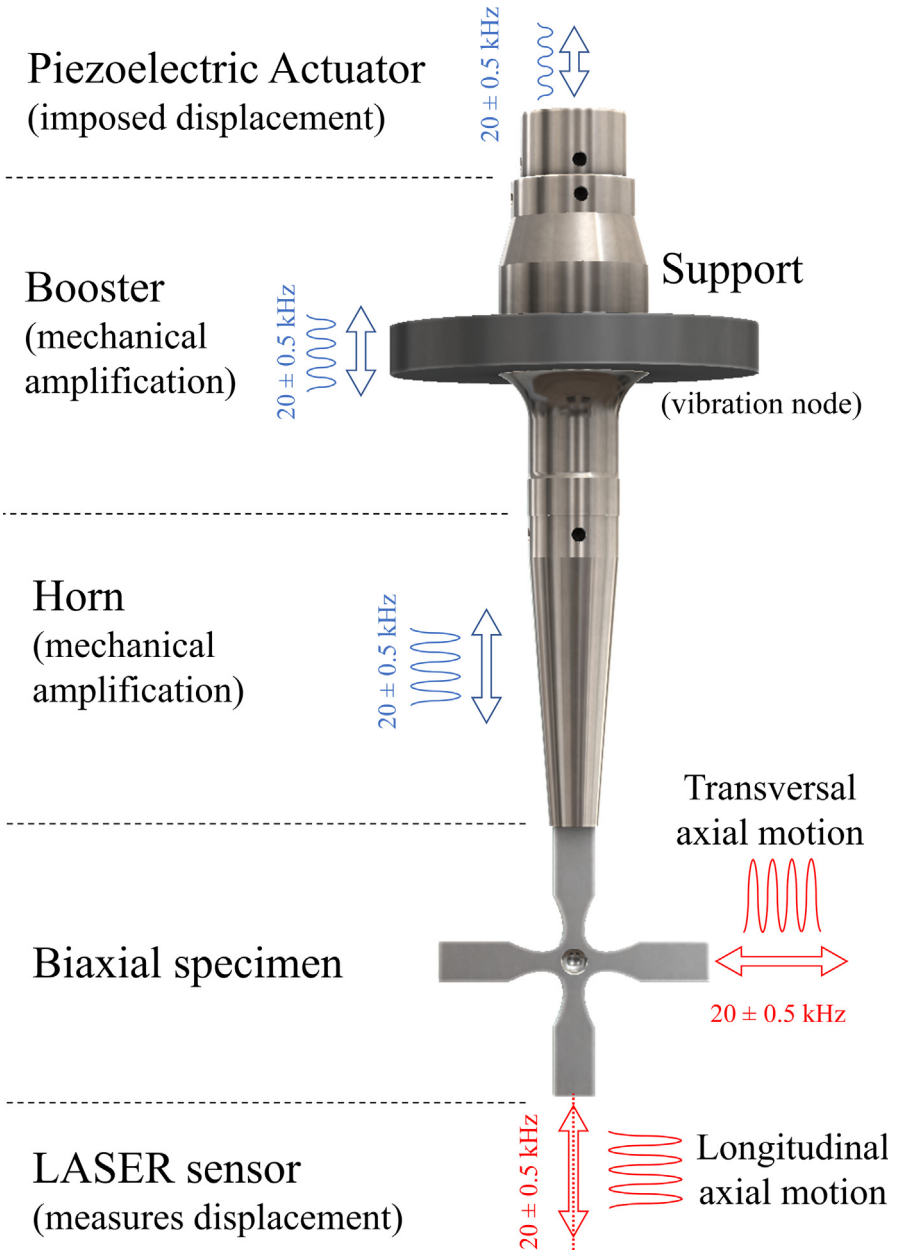

Fig. 1. VHCF testing machine resonant system components with biaxial specimen being tested (based on the machine from Lage et al. (2014)).

(Baptista et al., 2014; Makris et al., 2010). These specimens were developed for fatigue crack initiation studies, therefore feature a corner elliptical fillet between the specimen arms, in order to further reduce the stress concentration and to obtain a higher stress level at the specimen's centre (Baptista et al., 2016a).

The dimensions in Fig. 2 are determined from a set of equations available in Baptista et al. (2014), except the M2 thread that was added in the design of the

http://dx.doi.org/10.1016/j.heliyon.2017.e00466

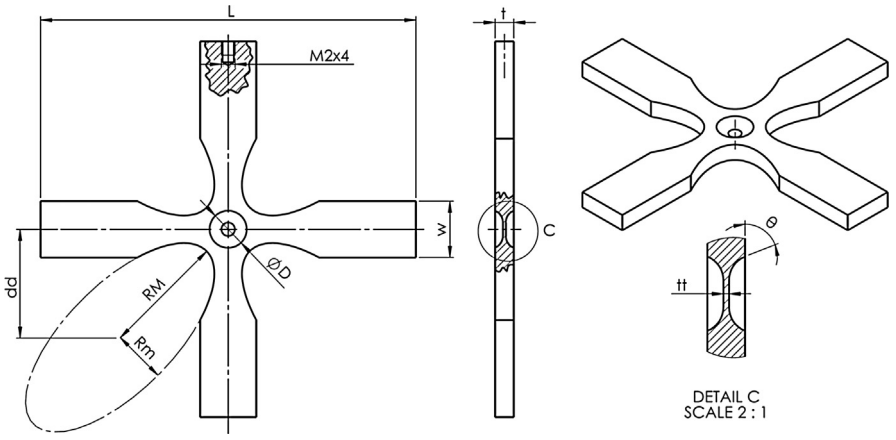

Fig. 2. Cruciform test specimen' shape.

current paper being presented to fix the specimen to the Horn of a VHCF fatigue testing machine like the one in Fig. 1. These authors recommend the use of an optimal geometry as a function of available standard sheet thicknesses, and used fixed values of L (200 mm) and w (30 mm) to constrain the optimisation problem.

Baptista et al. (2014) consider that the arms' thickness varies between 1 and 10 mm. In this paper, the largest thickness of 10 mm was chosen as starting point. The reason for this choice was not totally arbitrary, as the higher the thickness is, the higher is the bending stiffness, reducing the number of bending and torsional mode shapes before the axial mode shape we are looking for. However, in principle, any other assumption for the thickness could have been made, as long as one value is chosen. With this value in mind, the dimensions in Fig. 2 can be determined from equations (1) to (6) (Baptista et al., 2014):

$$RM(t) = -0.0379t^4 + 0.8223t^3 - 5.5749t^2 + 12.555t + 53.84 \quad (1)$$

$$Rm(t) = -0.0236t^3 + 0.3501t^2 - 0.5036t + 22.185 \quad (2)$$

$$dd(t) = -0.021t^4 + 0.4668t^3 - 3.248t^2 + 7.9452t + 46.224 \quad (3)$$

$$D(t) = 0.0342t^3 - 0.7936t^2 + 6.0398t + 4.5526, 4 \leq t \leq 10mm \quad (4)$$

$$\theta(t) = -0.7621t^3 + 15.484t^2 - 92.774t + 211.78, 4 \leq t \leq 10mm \quad (5)$$

$$tt(t) = 0.15t, t \geq 8\ mm \quad (6)$$

The results above are the optimal dimensions of a specimen that is not yet calibrated to be used in the VHCF regime, i.e., of a specimen that does not necessarily have a 20 ± 0.5 kHz axial natural frequency. Therefore, the design of the specimen with these dimensions will be called UD − Uncalibrated Design.

http://dx.doi.org/10.1016/j.heliyon.2017.e00466

3.2. Relationship between the natural frequencies and the dimensional scale factor

Let us assume that we want to determine the transverse natural frequencies of a beam with rectangular cross section. In this case, the angular natural frequencies can be determined from equation (7) (and most fundamental textbooks on vibration analysis will show it):

$$\omega_n = \left(\frac{k_n}{L}\right)^2 \sqrt{\frac{EI}{\rho A}} \tag{7}$$

where E is the Young's modulus of the material, ρ is its density, I is the second moment of area, A is the cross-sectional area of the L length beam and kn is a constant that depends on the mode number and boundary conditions. Considering, in this example, that the beam's cross section is rectangular, then the second moment of area I and area A can be written using equation (8):

$$I = \frac{1}{12}bh^3; A = bh \tag{8}$$

where b and h are the width and height (thickness) of the beam's cross section, respectively.

Therefore, for a matter of convenience of this demonstration and after some mathematical manipulation, equation (7) can be re-written in the form of equation (9):

$$\omega_n = \frac{h}{L^2}\sqrt{\frac{Ek_n^4}{12\rho}} \tag{9}$$

Now let us assume that we want to determine how much will the natural frequencies change when we scale down or up the beam by a factor s, i.e., $b' = s \cdot b$, $h' = s \cdot h$ and $L' = s \cdot L$. In this case, the new natural frequency can be determined from equation (10):

$$\omega_n^{'} = \frac{h^{'}}{L^{'2}}\sqrt{\frac{Ek_n^4}{12\rho}} = \frac{sh}{s^2L^2}\sqrt{\frac{Ek_n^4}{12\rho}} = \frac{1}{sL^2}\sqrt{\frac{Ek_n^4}{12\rho}} \tag{10}$$

or, in more simple terms, from equation (11):

$$\omega_n^{'} = \frac{1}{s}\omega_n \tag{11}$$

This result, equation (11), is very important in the design of specimens for VHCF. In practice, what it says is that if we scale up all the dimensions of an existing design by a scale factor of s, the natural frequencies will be scaled down in the same proportion. Since we want to have one of the axial mode shapes of the Calibrated Design (CD) cruciform specimen tuned at a certain natural frequency

http://dx.doi.org/10.1016/j.heliyon.2017.e00466

(in this case, 20 ± 0.5 kHz), we only need to determine the dimensional scale factor based on the natural frequency of the existing Uncalibrated Design (UD) earlier determined. In other words, and considering that the frequency is now in Hz for better convenience, the dimensional scale factor can be simply determined from equation (12) as:

$$s = \frac{f_{UD}}{f_{CD}} \tag{12}$$

where fCD = 20 kHz.

4. Methodology

The determination of the UD axial mode shapes' frequencies was done using Finite Element Analysis (FEA), considering a free-free configuration. Full details on the computational simulation setup (mesh, convergence analysis, etc.) are described in Wren (2017).

Wren (2017) used a COSMOS-based solver to perform two types of dynamic simulations: modal analysis and frequency response. The former was used to determine the frequencies of the T-T (in-phase) and C-T (out-of-phase) mode shapes. The latter was used to determine the relationship between the axial displacement at the specimens' arms' ends and the stress at their centres. This relationship is essential for the proof of concept, since these are the principles of operation of the machine from Lage et al. (2014), where the stress at the middle is determined from the measured displacement at the tip of the specimen through a LASER sensor.

The mesh was composed by 2nd order tetrahedral solid elements, with a global size of 2 mm and a size of 0.5 mm at the centre of the specimen. The specimen was modelled with the approximation that it is free-free suspended. This hypothesis is based on the fact that in the setup shown in Fig. 1, Booster, Horn and specimen are all resonating at their 1st axial mode shape, with a node in the middle and two anti-nodes at their ends.

In order to verify this hypothesis, Wren (2017) performed a simulation on the uniaxial test-specimen designed by Lage et al. (2014), also assuming free-free boundary conditions. The male thread from the uniaxial specimen, being an insert, was considered to be part of the horn so that it could be safely removed from the simulation. This analysis proved the initial assumption that the specimen could be modelled under free-free boundary conditions, at least if the 1st axial mode shape is the only one of interest. Furthermore, Wren (2017) performed a frequency response analysis to determine the relationship between the displacement at the tip of the uniaxial specimen and the stress at its centre. The results were compared to the analytical equations from Lage et al. (2014) and the FEA simulation validated

http://dx.doi.org/10.1016/j.heliyon.2017.e00466

(for the uniaxial test specimen). This gave insight on the FEA parameters to use for the biaxial case.

In the absence of analytical equations that relate the stress at the centre of the specimen and the displacement at the tip for the cruciform specimens, verification of the FEA model for the biaxial case was done by means of convergence and mesh independence analysis, as recommended in many textbooks, such as the ones from Zahavi (1992) or Radeş (2006). Once there was convergence and since models were validated for the uniaxial case, it is reasonable to assume that the FEA models for the cruciform specimens, which were based on the uniaxial one, are as equally valid. The frequency response FEA simulations considered a harmonic axial excitation at one end of the specimen, with amplitudes of 0.05 N, 0.1 N and 0.2 N. The amplitudes of the force required are very low, as expected, because the system will be resonating. These values strongly depend on damping, which was modelled to be a modal damping factor with an arbitrary value of 10^{-5}. This value is at the lower end of the damping factors measured in a same series alloy by (Colakoglu and Jerina, 2003). However, this choice does not affect the relationship between stress and displacement, which is what we are aiming at obtaining.

The material considered in the analysis is a 6082-T651 Aluminium alloy, a medium strength alloy with excellent corrosion resistance used in a diverse range of Engineering applications, including highly stressed structures that are subjected to in-plane biaxial or multiaxial loadings (Aalco, 2016; Karolczuk et al., 2015). The mechanical properties considered were a 72 GPa Young's modulus, a 0.33 Poisson's ratio and a 2700 kg/m^3 density (Makeitfrom, 2017).

5. Results

5.1. Determination of the UD and CD axial mode shapes' frequencies

The first two axial mode shapes of the UD specimen are shown in Fig. 3, where the scale factors presented were determined from equation (12). The resulting dimensions for the CD specimens are obtained from the application of the scale factors and are shown in Table 1.

One important observation from Fig. 3 is that these cruciform specimens will have two axial mode shapes (although only one is at 20 ± 0.5 kHz at any one time). Mode C-T corresponds to a situation where the axes are out-of-phase, i.e., when one of the axis is under traction and the other axis is under compression. In this case, the in-plane stresses are fully reversed. Mode T-T corresponds to a situation where both axes are in-phase, i.e., they both are either under traction or under compression simultaneously.

http://dx.doi.org/10.1016/j.heliyon.2017.e00466

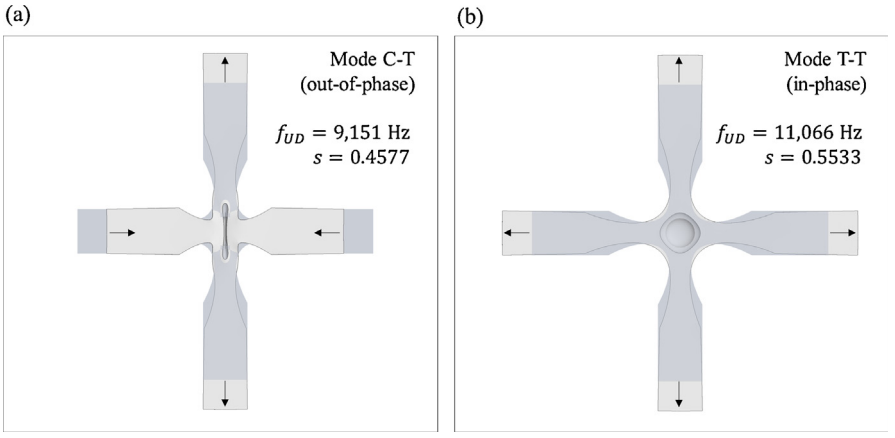

Fig. 3. Cruciform test specimen UD's first two axial mode shapes: C-T and T-T (deformation is exaggerated for better understanding). (a) C-T (out-of-phase) calibrated design. (b) T-T (in-phase) calibrated design.

Because these specimens are symmetric, they are designed to be tested under fully reversed cyclic loading (R = − 1) in both directions, as in other VHCF test methods (Lage et al., 2014).

Therefore, this paper also opens the possibility of expanding the study of in-plane biaxial fatigue with different phase loadings, as recently presented by Baptista et al. (2016b), to VHCF. The main difference, nonetheless, is that it is the specimen's design itself that influences the stress at the centre of the specimen

Table 1. Dimensions and estimated mode frequencies of the CD specimens after scaling.

	Uncalibrated Design UD	**Calibrated Design CD (C-T)**	**Calibrated Design CD (T-T)**
s	1	0.4577	0.5533
L(mm)	200	91.5	110.7
w(mm)	30	13.7	16.6
t(mm)	10	4.58	5.53
RM(mm)	65.2	29.8	36.1
Rm(mm)	28.9	13.2	16.0
dd (mm)	57.7	26.4	31.9
D(mm)	19.7	9.02	10.9
tt(mm)	1.50	0.687	0.830
θ (°)	70.6	70.6	70.6
f(Hz)	9,151 Hz (C-T) 11,066 Hz (T-T)	19,999 Hz	20,000 Hz

http://dx.doi.org/10.1016/j.heliyon.2017.e00466

rather than the way the loads are applied. In the case of the VHCF machine from Lage et al. (2014), the load is applied at a single coordinate (where the M2 thread is located in Fig. 2) in a single direction, as the underpinning principles are those used in SIMO (single-input-multiple-output) forced vibration and modal analysis.

It is important to mention that the M2 threaded hole (shown in Fig. 2 and used to fix the specimen to the horn through an M2 to M6 adaptor) has not been considered in the analysis. Firstly, this threaded hole can only be opened after the specimens are produced with the dimensions in Table 1, i.e., this is the only feature in the design that cannot be affected by the scale factor. Secondly, since a M2 to M6 threaded insert will have to be used to attach the specimen to the machine, the hole will be 'removed' from the specimen. Therefore, any changes in the CD frequencies are expected to be negligible, or at least not as determinant as other issues that will have to be considered during manufacturing.

5.2. Determination of the stresses at the centre of the cruciform test specimen

A correlation between the displacement of the specimen at one free end and the stress at the centre is needed to be determined if one is using a machine as the one depicted in Fig. 1. In such a machine, the displacement is measured in the axial direction with a LASER sensor at a free end of the specimen. The stress at the centre is then calculated from a correlation with the displacement at one arm's end that can be determined either analytically, numerically or experimentally.

The complexity of the geometry of this specimen suggests that the determination of analytical equations correlating the axial displacement with the stress at the centre can be a challenging task on its own account. To the authors knowledge, these have not been determined yet for the cruciform test specimens' design being used as a case study. Therefore, in the present work, FEA was used to find the relationship between the displacement at the tip and the stress at the centre, as detailed in Section 4.

Results are shown in Table 2, Fig. 4 and Fig. 5, where it can be seen that there is a linear relationship between the displacement at the tip and the stress at the centre. This is expected since the material model is linear. Once the model is calibrated, for example, from experimental tests using strain gauges or digital image correlation (DIC), these relationships can be used to determine different stress states at the centre of the specimen from imposed displacements. It is important, nonetheless, to have in mind that differences exist between the states of stress in the central part of cruciform specimens used for static tests and fatigue tests (Andrusca et al., 2014; Kuwabara et al., 1998; Leotoing and Guines, 2015; Van Petegem et al., 2016), which means that this calibration process may pose some challenges that need to be considered.

http://dx.doi.org/10.1016/j.heliyon.2017.e00466

Table 2. Relationship between the displacement at the arms' tips and the von Mises Stress at the centre.

	T-T Design		C-T Design	
$F(N)$	$d(\mu m)$	$\sigma(MPa)$	$d(\mu m)$	$\sigma(MPa)$
0	0	0	0	0
0.05	5.66	24.8	8.94	66.2
0.1	11.3	49.6	17.9	132.5
0.2	22.7	99.3	35.8	264.9

Specimen design C-T produces higher levels of von Mises stress than T-T for the same deformation. This is not a surprise, as its overall dimensions are smaller, namely at the centre of the specimen where the stresses are expected to be higher. The von Mises stress distribution in specimen C-T for the 0.1 N load case is illustrated, as an example, in Fig. 6. It can be observed how the stress level is almost constant on the specimen centre, while the stress at the arms is always at a significantly smaller level, even with the presence of a non-proportional stress with a phase shift of 180° (characteristic of case C-T). This is well in agreement with the intent from Baptista et al. (2014), which means that their design is suitable for VHCF, apart from a difference in the scale factor that must be determined somehow, for example following the procedure described in this paper.

The assumption that the specimens' design could be based on any initial thickness, namely one starting at 10 mm for the UD, proved to be feasible for this study. One important aspect to note is that the order of magnitudes of the displacements and stresses in Table 2 and Fig. 4 are consistent with the ones from Lage et al. (2014), which means that, once these specimens are manufactured, they can be tested in

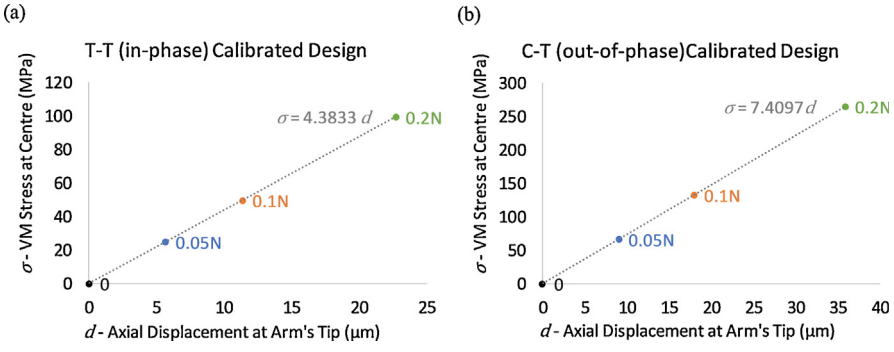

Fig. 4. Graphical representation of the relationship between the displacement at the arms' tips and the von Mises Stress at the centre. (a) T-T (in-phase) calibrated design. (b) C-T (out-of-phase) calibrated design.

http://dx.doi.org/10.1016/j.heliyon.2017.e00466

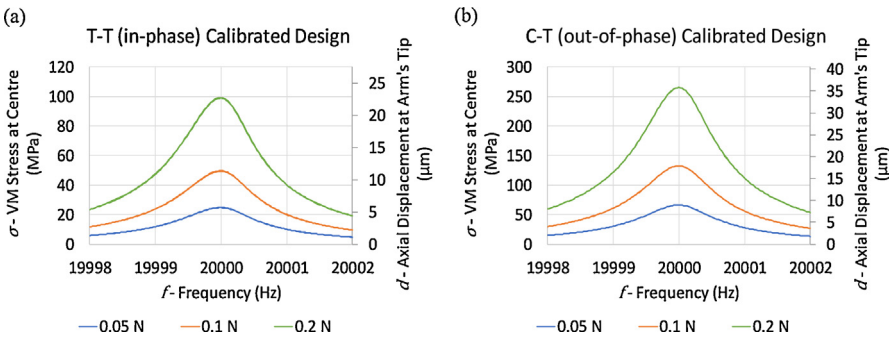

Fig. 5. Frequency response spectra of the von Mises Stress at the centre of the specimen and the axial displacement at the arm's tip. (a) T-T (in-phase) calibrated design. (b) C-T (out-of-phase) calibrated design.

VHCF machines such as the one from Lage et al. (2014). In this particular machine, a Branson DC222 transducer is used, which delivers a 20 μm peak-to-peak maximum displacement (Lage et al., 2012). The setup shown earlier in Fig. 1 shows a Booster and a tapered Horn, both designed to amplify the signals on a ratio of 2:1. This means that, at the end of the Horn, we can expect a maximum of 80 μm peak-to-peak displacement output as the driving excitation function of the specimen. If we now consider that the specimen is an underdamped system vibrating at steady-state and at resonance, both the amplification factor and transmissibility will be greater than 1. In other words, it is clear that we can get the displacement values shown in Table 2 and Fig. 4 from this machine with the

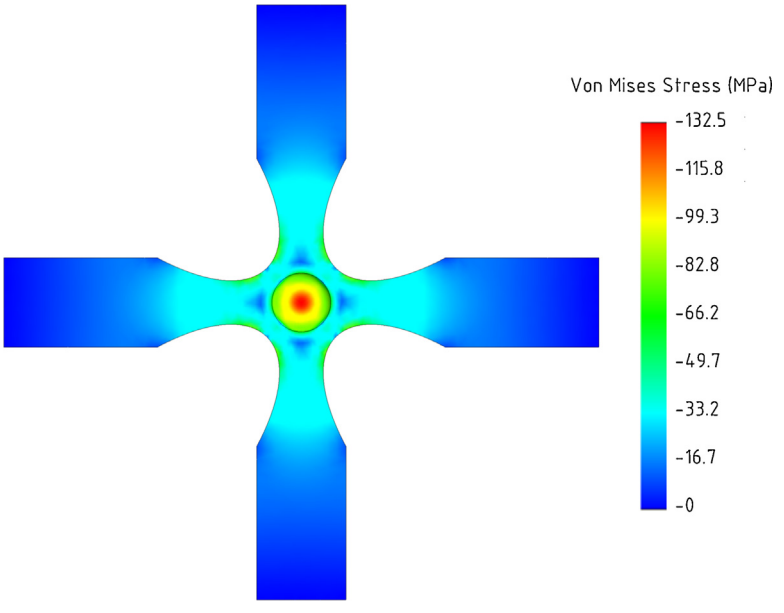

Fig. 6. Von Mises Stress distribution in the C-T Calibrated Design geometry for a 0.1 N axial harmonic excitation.

http://dx.doi.org/10.1016/j.heliyon.2017.e00466

designs presented in this paper. Regarding the stress amplitudes, this will depend on the material chosen. For Aluminium, the obtained stress levels are high enough and compatible with typical fatigue crack initiation/propagation shown in Al alloys in the VHCF regime (Höppel et al., 2011).

6. Conclusions

A numerical methodology to redesign existing cruciform test specimens so that they can be used in VHCF test machines was presented. These specimens are designed in such a way that, when attached through one end to the horn of the piezoelectric actuator, an in-plane biaxial state of stress is created at the centre of the specimen. It is expected that the methodology presented in this paper will be easily applied to other existing designs, namely cruciform designs or even new designs, that have not yet been considered in VHCF. This paper opens that possibility.

By contributing to bridging the gap between the sciences of modal analysis and fatigue, this work will help and encourage other researchers exploiting new capabilities in VHCF. Firstly, the way natural frequencies change with the application of a dimensional scale factor, although simple to demonstrate as shown in this paper, may not be so obvious for researchers who do not deal with modal analysis on a day-to-day basis. Secondly, the fact that the application of a load at a single coordinate (and in a single direction) can produce a biaxial state of stress (or even others) at a determined location of the specimen, may not also be so obvious, unless, and again, there is a background underpinned by modal analysis. There are many examples of biaxial specimens that were designed in the past, but all of them have something in common: they are designed so that at least 2 load pairs are applied in perpendicular directions (Abu-Farha et al., 2009; Baptista et al., 2015; Baptista et al., 2014; Bellett et al., 2011; Cláudio et al., 2014b; Kuwabara et al., 1998; Lebedev and Muzyka, 1998; Mönch and Galster, 1963; Shlyannikov et al., 2014; Smits et al., 2006). In VHCF this is no longer a key requirement, as it is shown in this paper: in principle, any design can be adapted to be used in an ultrasonic VHCF testing machine.

There are, however, many aspects that still require further research. Firstly, the manufacturing of the specimens may be a challenging one, as it is required that they have either the C-T (out-of-phase) or T-T (in-phase) mode shapes within a 20 $\pm$ 0.5 kHz natural frequency. This is not the only issue with manufacturing: how one can guarantee that the stress in one direction is the same as the stress in the other direction is just another challenge. Furthermore, how one can guarantee that two specimens, when manufactured and tested under the same conditions, actually develop the same stresses at the centre (for the same deformation), is another challenge. Another aspect that was not addressed in this paper is how neighbouring

http://dx.doi.org/10.1016/j.heliyon.2017.e00466

mode shapes influence the stress level at the centre of the specimen. It was considered that, since the other mode shapes are 'sufficiently' spaced from the axial-axial mode shape, then their influence is negligible, which is an assumption that is made in many other methods used in Modal Analysis (Ewins, 1984; Maia and eSilva, 1997). This means that there still is plenty of research work to be done with respect to the development of vibrating cruciform specimens to be used in VHCF, so that manufacturing conditions and experimental uncertainty are improved.

On the other hand, once specimens are manufactured, they must be calibrated. This can be done, for example, with a strain gauge rosette conveniently placed at the centre of the specimen. Another option (possibly a better option as long as the equipment is available) includes the use of Digital Image Correlation, which can be used in applications up to 100 kHz (Siebert and Crompton, 2013) or even more, and with resolutions around 1 micron and 0.01% strain according to some suppliers today (Dynamics, 2017). It would also be helpful if equations could be developed to predict the relationship between the expected stress at the centre and the axial displacement at the arm's tip, although this may be a complex task as it will depend on the specimens' shape.

Finally, how different initial thicknesses affect the performance of the resulting specimens in VHCF is something that should be studied in order to understand if there is one design that is more suitable for VHCF than others.

Declarations

Author contribution statement

Diogo Montalvão: Conceived and designed the experiments; Performed the experiments; Analyzed and interpreted the data; Contributed reagents, materials, analysis tools or data; Wrote the paper.

Andrew Wren: Conceived and designed the experiments; Contributed reagents, materials, analysis tools or data; Wrote the paper.

Funding statement

This research did not receive any specific grant from funding agencies in the public, commercial, or not-for-profit sectors.

Competing interest statement

The authors declare no conflict of interest.

http://dx.doi.org/10.1016/j.heliyon.2017.e00466

Additional information

No additional information is available for this paper.

References

Aalco, 2016. Aluminium Alloy 6082 - T6 ~ T 651 Plate. Aalco Metals Ltd. (Catalogue).

Abu-Farha, F., Hector, L., Khraisheh, M., 2009. Cruciform-shaped specimens for elevated temperature biaxial testing of lightweight materials. JOM 61, 48–56.

Andrusca, L., Goanta, V., Barsanescu, P.D., 2014. Optimizing the Shape and Size of Cruciform Specimens used for Biaxial Tensile Test. Appl. Mech. Mat. 658, 167–172.

Anes, V., Montalvao, D., Ribeiro, A., Freitas, M., Fonte, M., 2011. Design and instrumentation of an ultrasonic fatigue testing machine. Proceedings of VHCF5-5th International Conference on Very High Cycle Fatigue, 28-30 June 2011, Berlin, Germany.

Baptista, R., Claudio, R., Reis, L., Madeira, J.F.A., Guelho, I., Freitas, M., 2015. Optimization of cruciform specimens for biaxial fatigue loading with direct multi search. Theor. Appl. Fract. Mech. 80, 65–72.

Baptista, R., Cláudio, R.A., Reis, L., Guelho, I., Freitas, M., Madeira, J.F.A., 2014. Design optimization of cruciform specimens for biaxial fatigue loading. Frattura ed Integritá Strutturale 30, 118–126.

Baptista, R., Cláudio, R.A., Reis, L., Madeira, J.F.A., Freitas, M., 2016a. Numerical study of fatigue crack initiation and propagation on optimally designed cruciform specimens. Procedia Structural Integrity 1, 98–105.

Baptista, R., Cláudio, R.A., Reis, L., Madeira, J.F.A., Freitas, M., 2016b. Numerical study of in-plane biaxial fatigue crack growth with different phase shift angle loadings on optimal specimen geometries. Theor. Appl. Fract. Mech. 85, 16–25.

Bathias, C., 1999. There is no infinite fatigue life in metallic materials. FFEMS 22, 559–566.

Bathias, C., 2006. Piezoelectric fatigue testing machines and devices. Int. J. Fatigue 28, 1438–1445.

Bathias, C., De Monicault, J., Baudry, G., 2002. Automated piezoelectric fatigue machine for severe environments. Journal of ASTM International: Selected Technical Papers on Applications of Automation Technology in Fatigue and Fracture Testing and Analysis Fourth Volume, ASTM STP 1411, 3–15.

 http://dx.doi.org/10.1016/j.heliyon.2017.e00466

Bellett, D., Morel, F., Morel, A., Lebrun, J.L., 2011. A Biaxial fatigue specimen for uniaxial loading. Strain 47, 227–240.

Cláudio, R., Freitas, M., Reis, L., Li, B., Guelho, I., Antunes, V., Maia, J., 2014a. In-Plane Biaxial Fatigue Testing Machine Powered by Linear Iron-Core Motors. Journal of ASTM International: Selected Technical Papers on Application of Automation Technology in Fatigue and Fracture Testing and Analysis, ASTM STP, 1571.

Cláudio, R., Reis, L., Freitas, M., 2014b. Biaxial high-cycle fatigue life assessment of ductile aluminium cruciform specimens. Theor. Appl. Fract. Mech. 73, 82–90.

Colakoglu, M., Jerina, K., 2003. Material damping in 6061-T6511 aluminium to assess fatigue damage. FFEMS 26, 79–84.

Costa, P., Vieira, M., Reis, L., Ribeiro, A., De Freitas, M., 2017. New specimen and horn design for combined tension and torsion ultrasonic fatigue testing in the very high cycle fatigue regime. Int. J. Fatigue 103, 248–257.

Dynamics, D., 2017. Q-450 - High Speed DIC - Vibration Analysis and Transient Events. Accessed 12 October 2017 https://www.dantecdynamics.com/q-450-high-speed-dic-vibration-analysis-and-transient-events.

Ewins, D.J., 1984. Modal testing: theory and practice. Research studies press, Letchworth England.

Frederick, J., 1965. Ultrasonic engineering 1st Ed. John Wiley & Sons, New York.

Freitas, M., Anes, V., Montalvao, D., Reis, L., Ribeiro, A., 2011. Design and assembly of an ultrasonic fatigue testing machine. Proceedings of XXVIII GEF - Encuentro del Grupo Español de Fractura (Anales de Mecânica de la Fractura) 6-8 April 2011, Gijón, Spain.

Höppel, H.W., May, L., Prell, M., Göken, M., 2011. Influence of grain size and precipitation state on the fatigue lives and deformation mechanisms of CP aluminium and AA6082 in the VHCF-regime. Int. J. Fatigue 33, 10–18.

Karolczuk, A., Kurek, M., Łagoda, T., 2015. Fatigue life of aluminium alloy 6082 T6 under constant and variable amplitude bending with torsion. J. Theor. Appl. Mech. 53, 421–430.

Kuwabara, T., Ikeda, S., Kuroda, K., 1998. Measurement and analysis of differential work hardening in cold-rolled steel sheet under biaxial tension. Journal of Materials Processing Technology 80, 517–523.

Lage, Y., Freitas, M., Reis, L., Ribeiro, A., Montalvão, D., 2012. Instumentation of Ultrasonic High-Frequency Machine to Estimate Applied Stress in Middle

Section of Specimen. Proceedings of ICEM15-15th International Conference on Experimental Mechanics 22-27 July 2012, Porto, Portugal.

Lage, Y., Ribeiro, A., Montalvão, D., Reis, L., Freitas, M., 2014. Automation in strain and temperature control on VHCF with an ultrasonic testing facility. Journal of ASTM International: Selected Technical Papers in Application of Automation Technology in Fatigue and Fracture Testing and Analysis, ASTM STP 1571, 80–100.

Lebedev, A., Muzyka, N., 1998. Design of cruciform specimens for fracture toughness tests in biaxial tension. Strength Mater. 30, 243–254.

Leotoing, L., Guines, D., 2015. Investigations of the effect of strain path changes on forming limit curves using an in-plane biaxial tensile test. International Journal of Mechanical Sciences 99, 21–28.

Maia, N.M.M., eSilva, J.M.M., 1997. Theoretical and experimental modal analysis. Research Studies Press, Taunton.

Makeitfrom, 2017. 6082 (AlSi1MgMn, 3.2315, H30, A96082) Aluminum. [Accessed 10 June 2017] http://www.makeitfrom.com/material-properties/6082-AlSi1MgMn-3.2315-H30-A96082-Aluminum.

Makris, A., Vandenbergh, T., Ramault, C., Van Hemelrijck, D., Lamkanfi, E., Van Paepegem, W., 2010. Shape optimisation of a biaxially loaded cruciform specimen. Polym. Testing 29, 216–223.

Mönch, E., Galster, D., 1963. A method for producing a defined uniform biaxial tensile stress field. Brit. J. Appl. Phys. 14, 810–812.

Montalvão, D., Shengwen, Q., Freitas, M., 2014. A study on the influence of Ni–Ti M-Wire in the flexural fatigue life of endodontic rotary files by using Finite Element Analysis. Mater. Sci. Eng. C 40, 172–179.

Pyttel, B., Schwerdt, D., Berger, C., 2011. Very high cycle fatigue–Is there a fatigue limit? Int. J. Fatigue 33, 49–58.

Radeş, M., 2006. Finite element analysis. Printech.

Reis, L., Li, B., De Freitas, M., 2014. A multiaxial fatigue approach to Rolling Contact Fatigue in railways. Int. J. Fatigue 67, 191–202.

Shlyannikov, V., Tumanov, A., Zakharov, A., 2014. The mixed mode crack growth rate in cruciform specimens subject to biaxial loading. Theor. Appl. Fract. Mech. 73, 68–81.

 http://dx.doi.org/10.1016/j.heliyon.2017.e00466

Siebert, T., Crompton, M.J., 2013. Application of high speed digital image correlation for vibration mode shape analysis. Application of Imaging Techniques to Mechanics of Materials and Structures 4, 291–298.

Smits, A., Van Hemelrijck, D., Philippidis, T., Cardon, A., 2006. Design of a cruciform specimen for biaxial testing of fibre reinforced composite laminates. Compos. Sci. Technol. 66, 964–975.

Van Petegem, S., Wagner, J., Panzner, T., Upadhyay, M.V., Trang, T.T.T., Van Swygenhoven, H., 2016. In-situ neutron diffraction during biaxial deformation. Acta Materialia 105, 404–416.

Wren, A., 2017. Optimising an axial load specimen for biaxial very high cycle fatigue. BEng (Hons) in Engineering. Bournemouth University.

Zahavi, E., 1992. The finite element method in machine design. Prentice Hall.

 http://dx.doi.org/10.1016/j.heliyon.2017.e00466